Thermosensitive magnetic fluids

Andreas Kaiser, Thorsten Gelbrich and Annette M Schmidt

Institute for Organic Chemistry and Macromolecular Chemistry, Heinrich Heine University of Duesseldorf, Universitaetsstraße 1, D-40225 Duesseldorf, Germany

E-mail: schmidt.annette@uni-duesseldorf.de

Abstract
Magnetic core–shell particles were synthesized by the attachment of a polymeric brush on the surface of magnetite nanoparticles. The hybrid particles are well dispersible in good solvents for the polymeric shell and form thermoreversible magnetic fluids in carrier fluids with a critical solution behaviour. The thermoresponsive effect can be activated by the application of a high frequency electromagnetic field and may be useful for magnetic separation, recoverable catalysts and for drug release purposes.

1. Introduction

1.1. Background

Magnetic materials are key components in modern technology, with applications ranging from data storage to magnetic resonance imaging contrast agents. In this context, magnetic nanoparticles represent a critical link between current technology and future applications due to their unique size-dependent properties [1].

Dispersions of superparamagnetic particles in different carrier fluids, known as magnetic fluids [2], behave as liquids whose physical properties and flow behaviour can be controlled by external magnetic fields. Magnetic fluids are of high interest for basic research as well as for various applications. To date, they are in use for example as magnetically controlled seals and bearings and in loudspeaker coolings. A high potential for applications of magnetic fluids based on iron oxides is promised in the biomedical field [3]. Their use as improved MRI diagnostic contrast agents [4] and as a positioning tamponade for retinal detachment repair in eye surgery [5] has been reported. Ferrofluids are of high interest concerning magnetic drug targeting [6] and for cell separation methods [7].

In separation applications, magnetic fluids are of interest as they offer high surface area and can be functionalized to selectively discriminate between different molecular or cellular species. Present suggestions for nonmedical applications of magnetic fluids include the use of magnetic fluids as magnetically separable nanocatalytic systems that combine the advantages

of homogeneous and heterogeneous catalysis [8]. In these applications, a small particle size and effective dispersion stability by a suitable stabilization mechanism is required in order to achieve an optimum of specific binding or catalytic activity. In the same direction, however, these parameters complicate the magnetic separation of the particles.

The ability of ferrofluids to convert magnetic energy into heat by relaxational and hysteresis effects [9] has been known for a long time and has recently gained much attention for tumour therapy by magnetic hyperthermia [3].

Commonly used and commercially available magnetic fluids are dispersions of magnetic nanoparticles that are often stabilized by surface-active agents, acid and polymeric stabilizers. The steric stabilization mechanism involved is often of a dynamic nature, making it difficult to control the hydrodynamic diameter of the dispersed objects, and to prevent the formation of medium-sized (200–500 nm) agglomerates. In contrast, the functionalization of inorganic nanoscopic features with an irreversibly attached, covalently bound polymeric shell is a recent promising approach for the design of well-defined composite materials and dispersions [10], as this offers the opportunity to tailor dispersion properties like the minimum particle distance and the hydrodynamic particle volume. Additionally, an enhanced stability of such dispersions upon dilution, concentration or compositional changes of the dispersions may be expected.

A straightforward strategy for the synthesis of polymer-coated inorganic nanoparticles is the 'grafting-from' approach applied here by initiating the polymerization directly from the particle surface, resulting in a high number of end-attached polymer chains, often referred to as a polymeric brush [11]. Surface-initiated polymerization has been applied to various polymerization methods, including radical [12], cationic [13], anionic [14], ring-opening metathesis [15], and ring-opening polymerization (ROP) [16], and has been proved to be efficient in the coating of nanoparticles such as silica [17], starch granules [18], carbon nanotubes [19] and maghemite [20].

For the preparation of magnetic fluids, magnetic core/polymeric brush hybrid particles have the advantage to be instantly dispersible in good solvents for the polymeric shell without the addition of ancillary stabilizers [21–23]. In lieu thereof, the polymer arms serve as an irreversible attached steric stabilizer, leading to well-defined properties of the surfactant-free dispersion.

Our novel synthetic approach results in magnetic core–shell nanoparticles with a magnetite (Fe_3O_4) core and a covalently attached, stabilizing polymeric shell [22–24]. By dispersion of the hybrid particles in suitable nonpolar solvents, magnetic fluids are obtained without the use of stabilizing additives.

1.2. Motivation and scope

A number of polymeric materials are known for their ability to show a discontinuous change of properties due to temperature changes [25]. Some of these systems, e.g. thermoresponsive hydrogels and membranes, are based on the existence of critical solution temperatures (UCST or LCST) [26]. At a critical solution temperature, the solvation of polymer segments in a certain solvent is suddenly changed strongly due to the inversion of the free energy of mixing in the polymer/solvent system at that temperature. This may be due to entropic or enthalpic effects. The critical solution temperature is closely related to the theta temperature T_Θ of a polymer/solvent system, where the polymer–solvent interaction forces are just compensating those between the polymer segments, resulting in a coil-to-globule transition of the polymer chains at that temperature.

We present results on the synthesis and characterization of novel thermoreversible magnetic fluids based on magnetite (Fe_3O_4) coated with a covalently anchored, polymeric

shell of polystyrene (PS). The core–shell particles form stable dispersions in cyclohexane at temperatures above an upper critical solution temperature (UCST), while the particles precipitate below that temperature and can easily be separated by a magnet.

Thermoreversible stabilization of the particles offers an opportunity to combine dispersibility and quasi-homogeneous conditions for specific binding and catalytic activity, and easy magnetic separation at temperatures beyond the stabilizing conditions.

It is shown that it is possible to apply an alternating magnetic field as the trigger to induce thermal effects like solubility and/or permeability changes in the shell. This behaviour is of interest as well for medical applications in triggered drug release and may lead to a better understanding of the heat transfer mechanisms involved.

2. Experimental part

FeCl$_3$·6H$_2$O (Fluka) and FeCl$_2$·4H$_2$O (Baker) were used as received. 25% NH$_3$ aq. (Baker) and 37% HCl aq. (Riedel-de Haën) are of p. a. quality. Copper(I) bromide (CuBr, 98%), 4,4′-dinonyl-2,2′ bipyridine (dNbpy, 97%) and 2-bromo-2-methylpropionic acid (BMPA, 98%) were obtained from Sigma Aldrich and were used without purification. Styrene from Merck-Schuchardt was freshly distilled. Methanol was obtained in technical grade and used after distillation. Other solvents (toluene, benzene, cyclohexane, tetrahydrofurane) were purchased in analytical grade or higher. Toluene (p.a.) was dried over a molecular sieve (4 Å). All synthetic procedures were performed under inert (N$_2$ or Ar) atmosphere.

2.1. Synthesis

Fe$_3$O$_4$ nanoparticles were prepared by alkaline hydrolysis of ferrous and ferric chloride (molar ratio 1:2) aqueous solution using Cabuil and Massart's method [27]. The particles were washed several times with ammonium hydroxide solution (1.3%) and methanol. The freshly prepared particles were surface-functionalized by the addition of BMPA (1.67 mmol per gram Fe$_3$O$_4$) and stirring for 30 min at 50 °C. To remove untethered acid, the particles were washed extensively with methanol and degassed toluene. After adding an adequate amount of styrene and CuBr/dNbpy (1:2 mol mol^{-1}) as the catalytic system, the polymerization was started by heating the reaction mixture at 70 °C for 5 d under an argon atmosphere.

To obtain dispersions of the particles, toluene was added to the mixture and the resulting dispersions were centrifuged (2 min at 2000 r min^{-1}; relative centrifugative force: 380 g) to remove agglomerated material. Afterwards, the ferrofluids remained stable for several weeks and did not show any flocculation upon centrifugation or dilution. The ferrofluids were stored under argon in order to prevent the magnetite cores from oxidation to maghemite.

To investigate the composition of the hybrid particles by TGA, toluene was removed in vacuo, and the residue was dried carefully *in vacuo* to remove solvent and monomer residuals. To separate the polymeric arms from the magnetic core, a 10% dispersion in toluene was stirred vigorously with 1.0 M HCl aq. at room temperature until the black colour had changed to bright yellow. The organic phase was washed with brine and the polymer was isolated by precipitation in methanol. The polymeric fraction was dried and characterized by gel permeation chromatography (GPC).

For the preparation of thermosensitive magnetic fluids, Fe$_3$O$_4$@PS particles were transferred to cyclohexane by precipitation in methanol and washing several times with cyclohexane in order to remove residues of methanol.

2.2. Instrumentation

X-ray powder diffractograms were collected on a Huber G600 powder diffractometer (Cu Kα_1, quartz monochromator). Crystallite sizes have been calculated from line broadening according to the Scherrer equation [32] after correction for apparatus parameters. Elemental analysis (EA) of washed and carefully dried functionalized particles was carried out with a Perkin Elmer 2400 (series 2) CHN analyser. The degree of functionalization was calculated from the carbon content. Attenuated total reflection-infrared (ATR-IR) spectra were measured on a Nicolet FT-IR-55XB spectrometer equipped with a Specac Golden Gate Heated Diamond ATR Top Plate. Thermogravimetric analysis (TGA) experiments were performed with a Netzsch STA 449C. The samples were measured with a heating rate of 5 K min^{-1} under a nitrogen atmosphere in the temperature range 20–650 °C. The mass composition of dried hybrid particles was determined based on the weight loss by thermal decomposition of the polymer fraction in the temperature range 200–550 °C. The polymeric shell of the core shell particles was characterized by gel permeation chromatography (GPC) in tetrahydrofuran. The measurement system is based on a Waters 510 pump, three (300 × 8) mm^2 MZ Gel SDplus columns and a Waters 410 differential refractometer calibrated with polystyrene standards. Vibrating sample quasi-static magnetometry (VSM) was performed on a Micro Mag vibrating sample magnetometer from Princeton Measurements Corporation, with a field maximum of 1.3×10^6 A m^{-1}. Induction heating experiments were performed on a Huettinger High Frequency Generator TIG 5,0/300 equipped with a copper inductor ($l = 50$ mm, $d_I = 35$ mm, $n = 5$) and operating at 300 kHz. The maximum induction power was 5.0 kW. Dynamic Light Scattering (DLS) experiments were carried out with a Malvern HPPS-ET in the temperature range 17–75 °C. Hellma Suprasil precision cells 110-QS were used. The particle size distribution was derived from a deconvolution of the measured intensity autocorrelation function of the sample by the *general purpose mode* algorithm included in the *DTS* software. Each experiment was performed three times.

3. Synthesis of magnetic core–shell nanoparticles

In this work, we report the synthesis of hybrid core–shell particles with inorganic cores consisting of magnetite (Fe$_3$O$_4$) surface-functionalized by carboxylic acid-terminated polystyrene (PS) oligomers. The cores are selected to possess superparamagnetic behaviour, while the polymeric shell serves as a stabilizing layer and affords the preparation of stable particle dispersions. By choosing cyclohexane as the dispersion medium, magnetic fluids are obtained that possess a critical solution temperature leading to a thermoreversible volume transition of the hybrid particles. The UCST behaviour is attributed to the well-investigated presence of a theta temperature of PS in cyclohexane at 34.5 °C [28].

Surface-initiated polymerization is a relatively new pathway for the preparation of functional coatings and it has recently received much attention [21]. This technique is based on the growth of polymer molecules at the surface of a substrate *in situ* from surface-bound initiators. Consequently, covalently anchored end-tethered polymeric chains with a high grafting density on the particle surface are formed, commonly referred to as a polymeric brush [21]. For the presented hybrid particles, we chose the atom transfer radical polymerization (ATRP) for the surface-initiated polymerization of styrene from colloidal Fe$_3$O$_4$ particles [29], as it offers the advantage of a 'living'/controlled mechanism leading to ideally linear chains with low polydispersity (meaning uniform chain length of the individual chains) and good control on the molecular weight, combined with vast tolerance towards the reaction conditions [30].
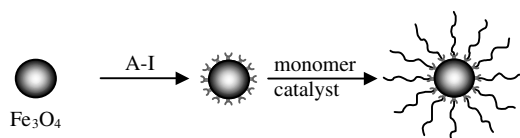
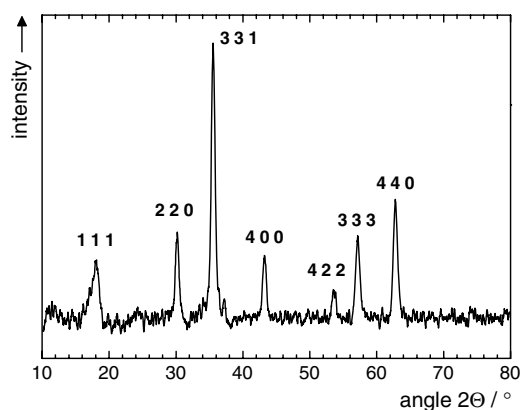**Scheme 1.** Synthesis scheme of magnetite-cored polymer brushes.

Figure 1. X-ray diffractogram of bare magnetite nanoparticles and correlated *hkl*-indices.

For the preparation of magnetic particle-cored polymeric brushes, we developed a three-step process. It consists of the precipitation of magnetite nanoparticles with a volume-average diameter of about 12 nm, the chemical modification of the particle surface by chemisorption of a functional carboxylic acid bearing a polymerization initiator, and finally grafting polymeric arms from the particle surface by the polymerization of a suitable monomer (see scheme 1).

To indicate the success of the synthetic pathway, careful characterization of the particles at different stages of the process was required. After alkaline precipitation, the Fe_3O_4 nanoparticles cores obtained were analysed by x-ray diffraction (XRD) analysis (see figure 1). No crystalline phase other than Fe_3O_4 was detected [31]. Using the Scherrer equation [32], we reproducibly calculated mean crystallite sizes of 12–13 nm from the line broadening of the signals. The value corresponds well with volume-average core size calculated from VSM of hybrid particle dispersions (see table 1). Furthermore, it was shown that the crystallite size does not change significantly upon functionalization or polymerization.

A surface functionalization of the particles with an ATRP initiator is achieved by heating the freshly prepared particle suspension in the presence of BMPA in order to chemisorb the acid on the particle surface.

The successful functionalization can be demonstrated by ATR-IR (see figure 2). Spectra of dried functionalized Fe_3O_4 nanoparticles show several characteristic peaks in the fingerprint region ($\nu = 1465, 1402, 1375, 1107$ cm^{-1}) also found in ATR-IR spectra of the free acid. In accordance with literature observations [33] we find a shift of 154 cm^{-1} of the vibrational absorption of the carbonyl double bond to lower wavenumbers and a decrease in intensity in comparison to the spectrum of the free acid ($\nu = 1702$ cm^{-1}) while the deformational stretching absorption of the (CO)–O–H group ($\nu = 1292$ cm^{-1}) vanishes, both indicating bidentate chemisorption via the carboxylate group [33].

Quantification of the particle surface functionality is possible by means of elemental analysis (EA) indicating a functionality f_{Ini} of 0.33 mmol g^{-1}.
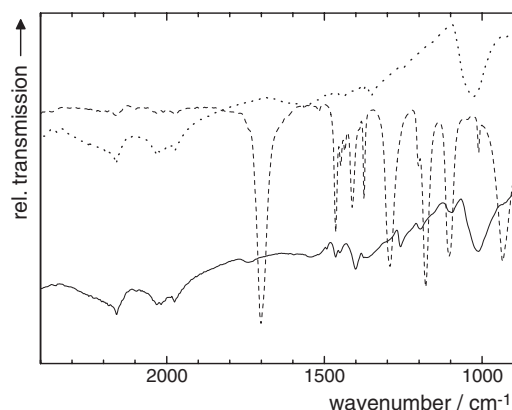
Figure 2. IR spectra of as-precipitated Fe_3O_4 particles (dotted line), BMPA (dashed) and surface-functionalized Fe_3O_4 particles (compact line).

Table 1. Composition of investigated Fe_3O_4@PS core–shell nanoparticles.

Sample[a]	μ_M[b] (mass%)	d_c[c] (nm)	M_n[d] (g mol^{-1})	M_w/M_n[e]	μ_{MF}[f] (mass%)	d_h[g] (nm)	SLP[h] (W g^{-1})
Fe_3O_4@PS59	59	11.7	6 110	1.33	1.5	54 ± 7	47.4
Fe_3O_4@PS52	52	11.6	6 400	1.42	0.67	59 ± 6	44.1
Fe_3O_4@PS49	49	11.5	10 300	1.36	0.97	77 ± 5	36.5
Fe_3O_4@PS37	37	13.3	10 800	1.72	0.46	82 ± 4	37.8
Fe_3O_4@PS25	25	13.4	22 200	1.58	0.76	87 ± 6	45.4
Fe_3O_4@PS23	23	11.5	27 800	1.18	0.41	103 ± 7	46.5

[a] Sample denotations: Fe_3O_4@PSμ_M.
[b] Fe_3O_4 content of dry hybrid particles (TGA).
[c] Core diameter (VSM) derived from initial susceptibility.
[d] Number-average molecular weight of polymer arms (GPC).
[e] Polydispersity index of polymer arms (GPC).
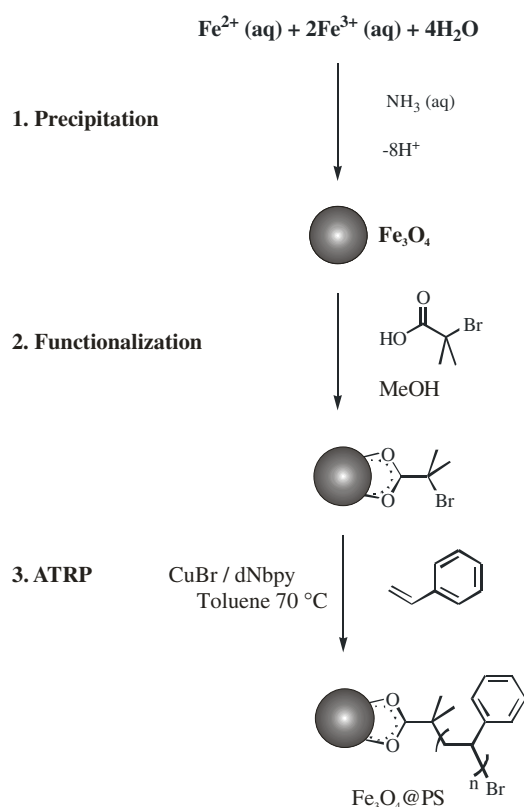[f] Fe_3O_4 content in toluene-based magnetic fluids (VSM).
[g] Hydrodynamic diameter of the core–shell particles in toluene (DLS).
[h] Specific loss power in toluene at 300 kHz, 5.0 kW.

For the preparation of the stabilizing polymer arms via surface-initiated ATRP the freshly synthesized and surface-functionalized nanoparticles are used as macroinitiators (see scheme 2). Grafting from ATRP of styrene is used to form a polymeric shell around the magnetic particles. The system used consists of CuBr as a catalyst and 4, 4′-dinonyl-2,2′-bipyridine as a ligand. Polymerization is carried out for 5 d at 70 °C in toluene.

The composition of the hybrid core–shell particles was investigated by means of thermogravimetrical analysis (TGA), giving the mass ratio of thermally decomposable polymeric fraction and Fe_3O_4 cores (see table 1). Thereafter, the hybrid particles contain up to 59 mass% of Fe_3O_4.

Additionally, the polymeric fraction was investigated by gel permeation chromatography (GPC) after acidolysis of the magnetic core. Biphasic conditions were chosen to prevent the polymeric chains from degradation by acidolysis, and linear PS was treated by the same method to ensure no significant change of the molecular weight by the treatment. The number-average molecular weights M_n range from 6 100 to 27 800 g mol^{-1} and show an increase with higher polymer content of the hybrid particles, showing the potential to alter the chain length by

$$Fe^{2+} (aq) + 2Fe^{3+} (aq) + 4H_2O$$

1. Precipitation

NH$_3$ (aq)

-8H$^+$

Fe$_3$O$_4$

2. Functionalization

MeOH

3. ATRP   CuBr / dNbpy
Toluene 70 °C

Fe$_3$O$_4$@PS

Scheme 2. Synthesis of Fe$_3$O$_4$@PS magnetic nanoparticles by surface-initiated ATRP of styrene.

varying the amount of added monomer. The polymer fractions showed polydispersity indices M_w/M_n of 1.2–1.7, in agreement with a fairly good control on the surface-initiated ATR polymerization.

Figure 3 shows the dependence of M_n on the mass ratio of PS and Fe$_3$O$_4$ content. A linear relationship is obtained, demonstrating that the functional particles serve as the initiating species for the polymerization. From the slope of the graph, the efficient initiation functionality f_s of the particles is calculated as (0.13 ± 0.02) mmol g^{-1}. Compared to the result for f_{Ini} as obtained by EA (see above), it can be concluded that not all of the surface-attached tertiary bromine groups are involved in the initiation process. At the same time, the axis intersection of the linear fit is close to zero, indicating the absence of significant amounts of initiating species in the crude monomer/solvent/catalyst mixture.

Taking into account the average surface area of approximately 470 nm^2 of an ideal spherical particle with a diameter of 12 nm, the result indicates a chain density of 0.8 chains nm^{-2} or approximately 400 polymer chains per particle.

4. Magnetic fluids based on Fe$_3$O$_4$@polystyrene

The hybrid particles obtained, consisting of a Fe$_3$O$_4$ core and a grafted polymeric shell, are well dispersible in toluene and benzene and are stable for several weeks. It is assumed that the grafted arms serve as the stabilizing component that prevents the particles from agglomeration
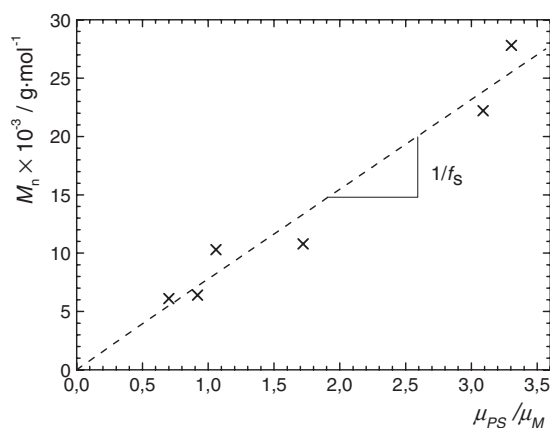
Figure 3. Molecular weight M_n of polymer arms versus mass ratio polystyrene/magnetite ($\mu_{PS} = 100\% - \mu_M$) of dry nanoparticles. The slope of the linear fit gives the chain density f_s per gram Fe$_3$O$_4$ with $f_s = (0.13 \pm 0.02)$ mmol g^{-1}.

due to van der Waals and magnetic dipole–dipole attractive forces. A thermoreversible dispersibility of the particles is detected in cyclohexane due to a critical solution behaviour of the polymeric shell (see below).

To support the architecture of the hybrid particles sketched in scheme 1, comparative experiments were carried out by polymerizing styrene in similar conditions, but in the presence of unfunctionalized Fe$_3$O$_4$ nanoparticles with and without the addition of 1,1-dimethylethyl (2-bromo-2-methylpropionate) as an alternative initiator. No peptization of the particles could be achieved in these experiments, showing the essential surface attachment of the polymer arms for effective stabilization.

The presented magnetic fluids are carefully characterized by quasi-static vibrating sample magnetometry (VSM), dynamic light scattering (DLS) and experiments on magnetic heatability.

The dispersions show superparamagnetic behaviour in VSM experiments with low coercitivity values (<0.6 kA m^{-1}) (figure 4) [34]. The saturation magnetization and initial susceptibility obtained from the experiments give information on the Fe$_3$O$_4$ content and the volume-average magnetite core size, respectively (see table 1). Fe$_3$O$_4$ contents between 0.41 mass% and 1.5 mass% are detected for the magnetic fluids in toluene. The good agreement with the core diameter of about 12 nm with XRD results indicates that the particle cores respond individually to the magnetic field.

In order to obtain more information on the hydrodynamic behaviour of the particle dispersions and to investigate the role of the stabilizing shell, DLS experiments were carried out in dilute toluene dispersions. We observed an increase of the hydrodynamic particle diameter d_h of Fe$_3$O$_4$@PS hybrid particles dispersed in toluene with the polymeric arm length given by M_n (figure 5). Compared to the theoretical relationship given by the simple model of ideally stretched polymer chains [26]

$$l_{max} = d_c + 2\left(\frac{M_n}{M_{Mono}}l_{Mono}\right) \tag{1}$$

with l_{max}: particle diameter according to the contour model, d_c: core diameter, M_n: number-average molecular weight of the polymer arms, M_{Mono}: molecular weight of the monomer unit, l_{Mono}: length contribution of a monomer unit according to the contour model, represented by
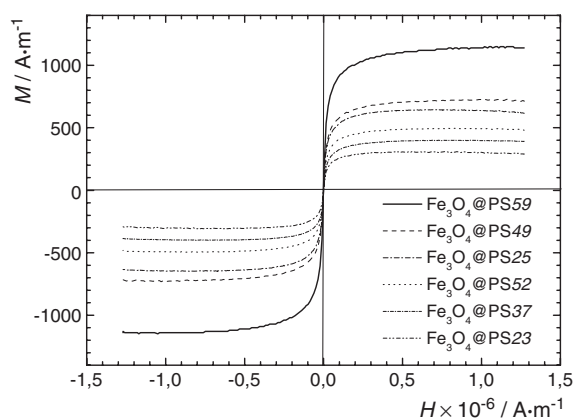
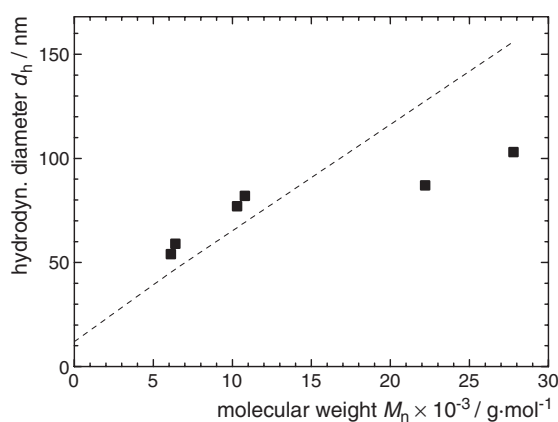**Figure 4.** Magnetization curves of Fe_3O_4@PS-based magnetic fluids in toluene.

Figure 5. Hydrodynamic diameter d_h (DLS) versus molecular weight M_n of the polymer arms (GPC) for Fe_3O_4@PS hybrid particles in toluene (■), compared to theoretical values for fully stretched polymer chains (dotted line).

the dotted line in figure 5, it is found that the discrepancy between experimental and theoretical values is smaller for Fe_3O_4@PS particles with short polymer chains, indicating that the chains are indeed in a highly stretched state. In comparison, the higher discrepancy for Fe_3O_4@PS hybrid particles leads to the assumption that a more coiled state is found for longer chains [11].

As pointed out above, the dispersibility of the hybrid brush particles is mainly ruled by the quality of the solvent used as the carrier fluid. If a solvent with lower solubility for the PS arms is chosen, a poor dispersibility is observed. Of particular interest are carrier fluids with a thermoreversible solubility with the polymeric shell, as is the case for cyclohexane with its theta temperature T_Θ for PS at 34.5 °C. Below T_Θ, the particles show a poor dispersibility due to the formation of polymer-mediated aggregates, whereas by rising the temperature above T_Θ, the polymer arms become more strongly solvated and act as effective steric stabilizers against the agglomeration of particles. A fully reversible upper critical solution behaviour (UCST) is observed. Consequently, the hybrid particles form stable magnetic dispersions in cyclohexane above a critical solution temperature T_c. As seen in figure 6, we observe the typical response of a magnetic fluid under the influence of a permanent magnet above T_c.
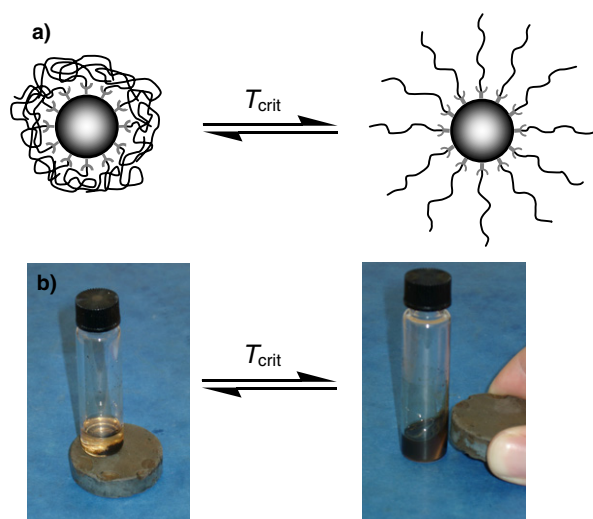
Figure 6. (a) Schematic behaviour of polymer brush particles in thermoreversible magnetic fluids. (b) Photographs of Fe_3O_4@PS37 in cyclohexane. The particles precipitate below T_c (at 20 °C, left-hand side). A particle dispersion is formed above T_c (at 50 °C, right-hand side) that reacts collectively under the influence of a permanent magnet.
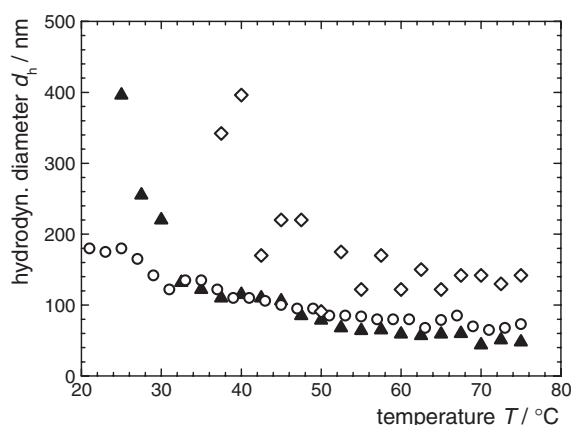

Figure 7. Hydrodynamic diameters versus temperature for Fe_3O_4@PS core–shell nanoparticles in cyclohexane: Fe_3O_4@PS59 (triangles), Fe_3O_4@PS37 (circles) and Fe_3O_4@PS25 (squares).

The corresponding critical temperature can be investigated in turbidity experiments, and transitions can be observed ranging from 35 up to 60 °C. Although it may be concluded that T_c increases with increasing arm length and particle concentration, the exact dependence is under investigation.

For cyclohexane-based dilute particle dispersions of 0.1 mg ml^{-1}, the transition between an agglomerated state and dispersion of single particles upon temperature rise is shown in DLS experiments.

The results of the peak diameter against temperature are presented in figure 7 for three Fe_3O_4@PS samples in cyclohexane. Below 30–40 °C, particle diameters of some hundred nanometres are obtained that can be attributed to the formation of agglomerates. At higher
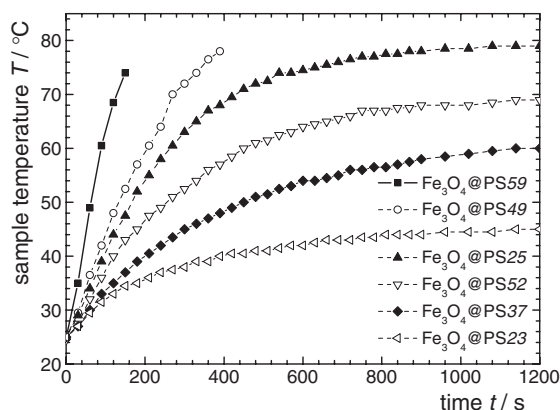
Figure 8. Magnetic heating measurements of magnetic fluids based on Fe_3O_4@PS hybrid particles in toluene.

temperatures, the diameter decreases until particle sizes are observed which are in agreement with values found in toluene at ambient temperature, or slightly higher in the case of Fe_3O_4@PS25.

Magnetic fluids hold the potential to convert magnetic energy into heat due to relaxational and hysteresis effects [2, 3]. We are interested in this property, as it offers the opportunity to activate thermal property changes within an accordingly designed materials system. In this context, the specific loss power of Fe_3O_4@PS dispersions in toluene and cyclohexane are investigated. A vacuum isolated glass sample container is placed in the middle of an induction coil. A high frequency magnetic field of 300 kHz is applied to the sample and the sample temperature versus time is measured (see figure 8). At the beginning of the measurement, a linear relationship between temperature and time is observed. The slope decreases with time due to heat exchange with the environment. Higher mass contents of the fluids lead to faster heating. Taking into account the heat capacity and the magnetite content of the system, the specific loss power (SLP) is calculated from the initial slope. SLP values between 36.5 and 47.4 W g^{-1} are found, with no direct correlation to the shell thickness or the magnetite content of the fluids. This may be attributed to the expected Neelian relaxation mechanism [35], independent from the magnetic core's outer mobility, and thus the hydrodynamic volume of the hybrid particles.

Accordingly magnetic heating curves are obtained for particle dispersions in cyclohexane, with no influence of the thermal transition on the curve being observed. It may be assumed that the magnetic heatability of the particles is not affected by the state of the polymeric shell.

Future experiments on the incorporation of catalytically active groups to the polymeric shell will show if magnetic dispersions based on Fe_3O_4@PS hybrid particles can be of use in switchable catalytic systems.

5. Recent achievements in thermosensitive magnetic fluids

5.1. Shell polymers and polymerization mechanisms

Our former works [22–24] show that by applying the synthetic pathway to other polymeric systems, magnetic nanoparticles with a tailored polymeric shell concerning composition and thickness are accessible. We realized hybrid magnetic particles with shells composed of poly(2-methoxyethyl methacrylate) (PMEMA), being dispersible in polar solvents like DMF
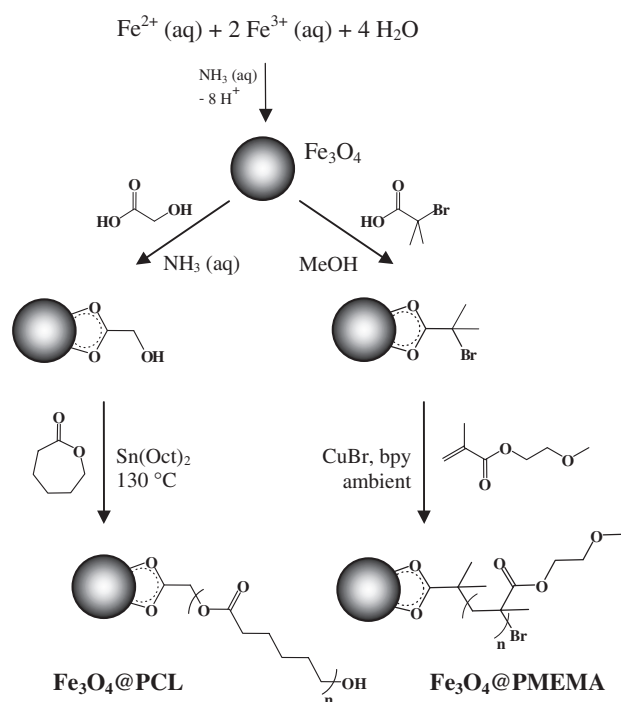
Scheme 3. Synthetic pathways for the preparation of Fe$_3$O$_4$@PCL and Fe$_3$O$_4$@PMEMA magnetic polymer brushes. Reproduced with permission from reference [24]. Copyright 2006 Oldenbourg.

and DMSO, and of poly(ε-caprolactone) (PCL), dispersible in less polar organic solvents like toluene and chloroform (see scheme 3).

PCL-coated magnetite nanoparticles (Fe$_3$O$_4$@PCL) were prepared by surface-initiated ring-opening polymerization of ε-caprolactone monomer [22]. PCL was chosen as the shell material due to its solution properties and the well-known polymerization behaviour allowing direct control of the polymeric arm length. An additional feature is the good biocompatibility of PCL, being attractive for biomedical applications.

For the preparation of magnetite particles coated with PMEMA (Fe$_3$O$_4$@PMEMA), a synthetic route via ATRP was applied [23]. PMEMA shows solubility in polar solvents like DMF and DMSO, and MEMA is copolymerizable by ATRP with various (meth)acrylates and (meth)acrylamides.

Careful characterization of the particles at different stages of the process by XRD, ATR-IR, TGA, VSM and TEM has been described in detail recently [22, 23], together with the results of the investigation of the polymeric fraction by analytical methods in solution (^{1}H-NMR and GPC) after acidolysis of the magnetic core. Table 2 summarizes the composition of various core–shell particles with a Fe$_3$O$_4$ mass fraction μ_M between 10% and 40%. The findings indicate a direct linear correlation between the polymer arm length as given by the molecular weight and the polymer-to-magnetite ratio that can be assigned to the surface-initiated growth of the chains for both types of hybrid particle. The slope of the linear plot μ_{PCL}/μ_M against M_n leads to a chain density f_s of 0.83 mmol g^{-1} for particles of the Fe$_3$O$_4$@PCL-type, while for Fe$_3$O$_4$@PMEMA particles, a chain density of 0.26 mmol g^{-1} is calculated.

TEM images of DMF-cast Fe$_3$O$_4$@PMEMA particles (see figure 9) confirm the architecture of the obtained core–shell particles. Strongly contrasting, nearly spherical
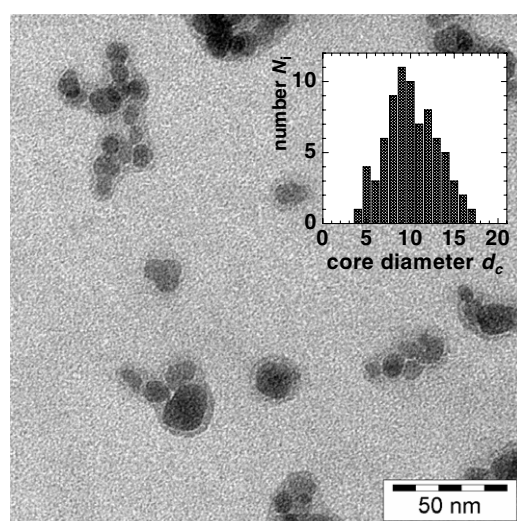
Figure 9. TEM image of Fe_3O_4@PMEMA18 hybrid particles. Inset: core size distribution (TEM, $n = 76$). Reproduced with permission from reference [23]. Copyright 2006 American Chemical Society.

Table 2. Composition of investigated Fe_3O_4@PCL and Fe_3O_4@PMEMA core–shell nanoparticles.

Sample[a]	μ_M[b] (mass%)	d_c[c] (nm)	M_n[d] (g mol^{-1})	M_w/M_n[e]	μ_{MF}[f] (mass%)
Fe_3O_4@PCL40	40	12.4	1 500	3.85	3.5
Fe_3O_4@PCL25	25	12.1	3 500	2.25	1.3
Fe_3O_4@PCL20	20	12.2	4 900	2.06	0.67
Fe_3O_4@PCL13	13	11.9	7 100	2.07	0.57
Fe_3O_4@PCL10	10	12.5	12 300	1.89	0.39
Fe_3O_4@PMEMA43	43	11.8	11 000	1.85	3.0
Fe_3O_4@PMEMA30	30	12.9	16 800	3.09	1.0
Fe_3O_4@PMEMA18	18	n. d.	30 900	2.16	n. d.
Fe_3O_4@PMEMA16	16	12.2	35 100	2.15	0.48

[a] Sample denotations: Fe_3O_4@polymer μ_M.
[b] Fe_3O_4 content of dry hybrid particles (TGA).
[c] Core diameter (VSM) derived from initial susceptibility.
[d] Number-average molecular weight of polymer arms (GPC).
[e] Polydispersity index of polymer arms (GPC).
[f] Fe_3O_4 content in toluene-based magnetic fluids (VSM).

magnetite cores with a number-average diameter of 10.8 nm can be clearly distinguished from a closed polymeric shell. Within the observed small particle aggregates that are possibly formed during sampling, the single magnetite cores are mostly visibly separated by a PMEMA shell. We estimate a polymer layer thickness of 3–5 nm, independent of the individual core size.

The dispersion properties of the magnetic fluids obtained were studied by DLS [24], and we found an increase of the hydrodynamic particle diameter with the polymeric arm length for both types of magnetic brush particle in dispersion (see figure 10). While the main peak of the number-average diameter distribution can be assigned to particularly dispersed particles, a considerable amount of agglomerates is detected as a shoulder or high diameter fraction for particles with high polymer content and long chains. This is predominantly the case in
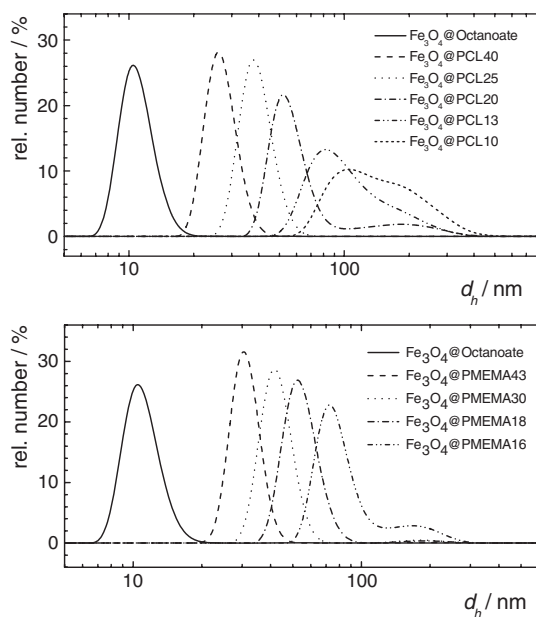
Figure 10. Hydrodynamic particle diameter d_h distribution of Fe_3O_4@PCL particles dispersed in toluene (a) and Fe_3O_4@PMEMA particles in DMF (b). Reproduced with permission from [24]. Copyright 2006 Oldenbourg.

dispersions of Fe_3O_4@PMEMA16, Fe_3O_4@PCL13 and Fe_3O_4@PCL10. It can be assumed that the agglomeration occurred due to entanglement of the polymeric arms and/or partial crosslinking reactions between individual particles during polymerization at high monomer conversions.

5.2. Magnetic heating

In magnetic heating experiments, a similar behaviour was observed as described for Fe_3O_4@PS dispersions in toluene (see section 3). From the initial slope, dT/dt is determined and plotted against the magnetite content of the fluids (see figure 11).

A linear relationship between the loss power $c_p \cdot dT/dt$ and μ_M is observed. The slope of the graphs is the specific loss power (SLP). For Fe_3O_4@PMEMA-based fluids, the SLP of the magnetite cores is calculated to the 51.9 W g^{-1} and for the Fe_3O_4@PCL-based fluids 27.5 W g^{-1} is found. These values are independent of the shell thickness, indicating a *Néel*ian relaxation mechanism [35]. The difference between the SLP of PMEMA- and PCL-based materials may be attributed to different core batches used in the synthesis of the two systems.

5.3. Magneto- and thermoresponsive effects

Thermoreversible magnetic fluids are obtained by dispersing Fe_3O_4@PMEMA particles in methanol, and similarly of Fe_3O_4@PCL in dimethylsulfoxide (DMSO). A similar behaviour is observed as for Fe_3O_4@PS particles in cyclohexane due to the existence of a UCST.

For the PMEMA-capped particles an inverse dependence of T_c on the molecular weight can be detected. T_c varies between 21 and 39 °C. Figure 12 shows the corresponding turbidity experiments.
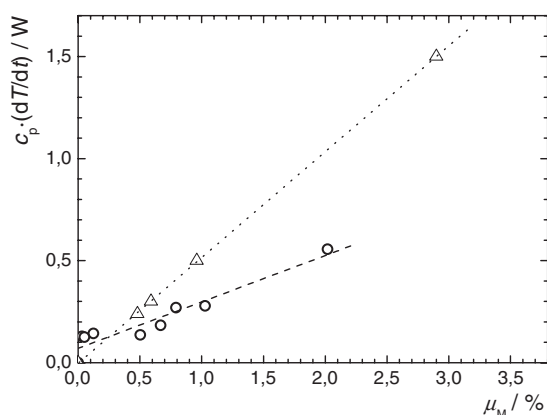
Figure 11. Magnetic heating of magnetic fluids: dotted line (triangle) Fe_3O_4@PMEMA nanoparticles in DMF; dashed line (circles): Fe_3O_4@PCL in toluene.
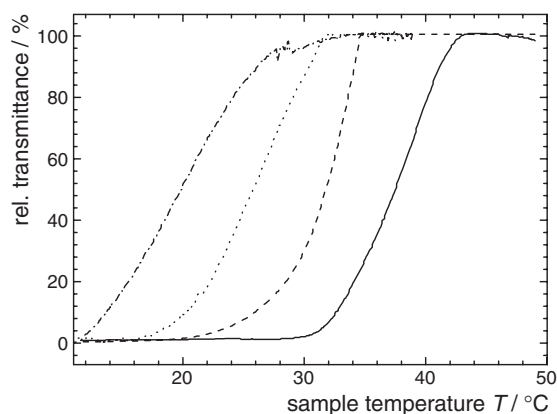

Figure 12. Relative transmittance versus sample temperature T of Fe_3O_4@PMEMA suspensions in methanol in turbidity experiments; compact line: Fe_3O_4@PMEMA43, dashed: Fe_3O_4@PMEMA30, dotted: Fe_3O_4@PMEMA18, dash–dotted: Fe_3O_4@PMEMA16. Reproduced with permission from [23]. Copyright 2006 American Chemical Society.

A proof of concept, that it is possible to induce the release of a probe from suspensions of loaded particles by magnetic heating, is given for Fe_3O_4@PCL particle dispersions in DMSO. This is shown in figure 13 for Fe_3O_4@PCL10 (1 mass% in DMSO) loaded with the solvatochromic dye 1-methyl-4-[2-(4-oxocyclohexa-dienylidene)ethylidene]-1,4-dihydropyridine (p-MOED) (1.7 mass% load). A clear change of colour due to the release of the dye upon passing the UCST is observed between 36 and 42 °C. It is obvious that this concept may be of interest for drug release applications.

6. Summary

This report describes the synthesis of nanoscopic Fe_3O_4-cored polymeric brushes and the properties of novel thermoreversible magnetic fluids based thereon.

The synthesis has successfully been performed by surface functionalization of Fe_3O_4 nanoparticles and subsequent surface-initiated ATRP of styrene. We verified the synthetic
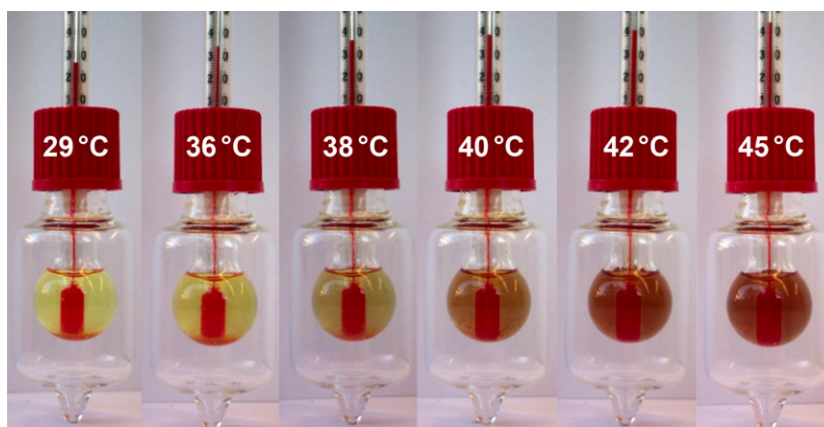
Figure 13. Release of p-MOED from loaded Fe_3O_4@PCL hybrid particles in DMSO by magnetic heating (see text).

pathway and the proposed architecture of the particles by careful characterization of the hybrid materials. A high grafting density and an adjustable shell thickness given by M_n of the tethered chains are found.

The hybrid particles can be peptized in good solvents for the polymeric shell, like toluene or benzene, up to 1.5 mass%. In these magnetic fluids, the polymeric brush shell serves as stabilizing layer, and no additional stabilizing agent is needed. The hydrodynamic diameter d_h of the 12 nm Fe_3O_4 cores can thus be tailored by the polymer arm length M_n. The resulting ferrofluids show superparamagnetic behaviour in quasi-static magnetization experiments and magnetic heatability in an oscillating magnetic field.

A thermoreversible dispersibility is observed in cyclohexane with a UCST-like behaviour around 34 °C. The thermoreversibility can be attributed to the theta temperature of PS in cyclohexane at 34 °C.

The presented synthetic pathway was recently applied to other monomers suitable for surface-initiated polymerization, and offers a method to prepare ferrofluids with tailored properties by the introduction of a well-defined, surface-attached polymeric stabilization layer. We realized hybrid particles that are well dispersible in DMSO and DMF, or toluene and chloroform, respectively. Thermoreversible dispersibility with UCST behaviour is found for Fe_3O_4@PMEMA particles in methanol, and for PCL-coated particles in DMSO. The effect has been shown to be useful for the release of a solvatochromic probe from loaded particles by exposition to an alternating magnetic field.

The presented combination of thermoresponsive polymers with the properties of magnetic fluids, together with tailorable hydrodynamic diameter and critical temperature, may contribute to the development of easily recoverable polymer-supported magnetic separation kits and catalytic systems. Additionally, they are of interest as model fluids for the examination of relaxation behaviour and magnetic particle interactions.

Acknowledgments

References

[1] Craik D 1995 *Magnetism—Principles and Applications* (Chichester: Wiley)
[2] Berkovsky B M and Bashtovoy V 1996 *Magnetic Fluids and Applications Handbook* (New York: Begell House)
   Blums E, Cebers A and Mairov M M 1997 *Magnetic Fluids* (Berlin: Walter de Gruyter)
[3] Andrä W 1998 *Magnetism in Medicine* ed W Andrä and H Nowak (Berlin: Wiley–VCH)
   Pankhurst Q A, Connolly J, Jones S K and Dobson J 2003 *J. Phys. D: Appl. Phys.* **36** R167–81
   Tartaj P, Morales M P, Veintemillas-Verdaguer S, Gonzáles-Carreno T and Serna C J 2003 *J. Phys. D: Appl. Phys.* **36** R182–97
   Berry C C and Curtis A S G 2003 *J. Phys. D: Appl. Phys.* **36** R198–211
[4] Babes L, Denizot B, Tanguy G, Le Jeune J J and Jallet P 1999 *J. Colloid Interface Sci.* **212** 474
[5] Dayley J P, Philipps J P, Li C and Riffle J S 1999 *J. Magn. Magn. Mater.* **194** 140
[6] Alexiou C, Arnold W, Hulin P, Klein R, Schmidt A, Bergemann C and Parak F G 2001 *Magnetohydrodynamics* **37** 3
[7] Roath S 1993 *J. Magn. Magn. Mater.* **122** 329
[8] Lu A H, Schmidt W, Matoussevitch N, Bönnemann H, Spliethoff B, Tesche B, Bill E, Kiefer W and Schüth F 2004 *Angew. Chem.* **116** 4403–6
   Lu A H, Schmidt W, Matoussevitch N, Bönnemann H, Spliethoff B, Tesche B, Bill E, Kiefer W and Schüth F 2004 *Angew. Chem. Int. Edn* **43** 4303–6
   Teunissen W, de Groot F M F, Geus J, Stephan O, Tence M and Colliex C 2001 *J. Catal.* **204** 169–74
[9] Brown W F Jr 1959 *J. Appl. Phys. Suppl.* **30** 130S
[10] Carrot G, Rutot-Houze D, Pottier A, Degée P, Hilborn J and Dubois P 2002 *Macromolecules* **35** 8400–4
   El Harrak A, Carrot G, Oberdisse J, Eychenne-Baron C and Boué F 2004 *Macromolecules* **37** 6376
   Pyun J, Shijun J, Kowalewski T, Patterson G D and Matyjaszewski K 2003 *Macromolecules* **36** 5094
   Fendler J H 1996 *Chem. Mater.* **8** 1616
[11] Rühe J 2004 *Polymer Brushes* ed R C Advincula, W J Brittain, K C Caster and J Rühe (Weinheim: Wiley–VCH) p 18
   Zhao B and Brittain W J 2000 *Prog. Polym. Sci.* **25** 677
   Pyun J, Kowalewski T and Matyjaszewski K 2003 *Macromol. Rapid Commun.* **24** 1043–59
[12] Prucker O and Rühe J 1998 *Macromolecules* **31** 592
[13] Jordan R, West N, Ulman A, Chou J M and Nuyken O 2001 *Macromolecules* **34** 1606–11
[14] Yee C, Scotti M, Ulman A, White H, Rafailovich M and Sokolov J 1999 *Langmuir* **15** 4314
[15] Weck M, Jackiw J J, Rossi R R, Weiss P S and Grubbs R H 1999 *J. Am. Chem. Soc.* **121** 4088
[16] Choi I S and Langer R 2001 *Macromolecules* **34** 5361
   Husemann M, Mecerreyes D, Hawker C J, Hedrick L J, Shah R and Abbott N L 1999 *Angew. Chem. Int. Edn* **38** 647
[17] Yoon K R, Koh Y-J and Choi I S 2003 *Macromol. Rapid Commun.* **24** 207–10
   Joubert M, Delaite C, Bourgeat-Lami E and Dumas P 2004 *J. Polym. Sci.* A **42** 1976–84
[18] Yoon K R, Lee Y-W, Lee J K and Choi I S 2004 *Macromol. Rapid Commun.* **25** 1510–3
[19] Dubois P, Krishnan M and Narayan R 1999 *Polymer* **40** 3091
[20] Flesh C, Delaite C, Dumas P, Bourgeat-Lami E and Duguet E 2004 *J. Polym. Sci.* A **42** 6011
[21] Vestal C R and Zhang Z J 2002 *J. Am. Chem. Soc.* **124** 14312–3
   Matsuno R, Yamamoto K, Otsuka H and Takahara A 2003 *Chem. Mater.* **15** 3–5
[22] Schmidt A M 2005 *Macromol. Rapid Commun.* **26** 93–7
[23] Gelbrich T, Feyen M and Schmidt A M 2006 *Macromolecules* **3** 3469–72
[24] Gelbrich T, Feyen M and Schmidt A M 2006 *Z. Phys. Chem.* **220** 41–9
[25] Tanaka T 1978 *Phys. Rev. Lett.* **40** 820
   Aoyagi T, Miyata F and Nagase Y 1994 *J. Control. Release* **32** 87
[26] Elias H G 2001 *Makromoleküle Band 2: Physikalische Strukturen und Eigenschaften* (Weinheim: Wiley–VCH)
[27] Massart R and Cabuil V 1987 *J. Chem. Phys.* **84** 967–73
[28] Saeki S, Kuwahara N, Konno S and Kaneko M 1973 *Macromolecules* **6** 246
[29] von Werne T and Patten T E 2001 *J. Am. Chem. Soc.* **123** 7497–505
   Ohno K, Koh K, Tsujii Y and Fukuda T 2003 *Angew. Chem.* **115** 2857–60
   Ohno K, Koh K, Tsujii Y and Fukuda T 2003 *Angew. Chem. Int. Edn* **42** 2751–4

Duan H, Kuang M, Wang D, Kurth D G and Möhwald H 2005 *Angew. Chem.* **117** 1745–8

Duan H, Kuang M, Wang D, Kurth D G and Möhwald H 2005 *Angew. Chem. Int. Edn* **44** 1717–20

Chen X, Randall D P, Perruchot C, Watts J F, Patten T E, von Werne T and Armes S P 2003 *J. Colloid Interface Sci.* **257** 56–64

[30] Matyjaszewski K and Davis T P 2002 *Handbook of Radical Polymerization* (New York: Wiley–Interscience)

[31] Fleet M E 1981 *Acta Crystallogr.* B **37** 917–20

[32] Scherrer P 1918 *Nachr. Ges. Wiss. Göttingen, Math.-Phys. Kl.* **2** 98

[33] Rocchiccioli-Deltcheff C, Franck R, Cabuil V and Massart R 1987 *J. Chem. Res.* 1209–30

[34] Rosensweig R E 1985 *Ferrohydrodynamics* (New York: Cambridge University Press)

[35] Néel M L 1949 *Ann. Geophys.* **5** 99